Interdiffusion in $L1_2$-Ni$_3$Al Alloyed with Re

N. Garimella, M. Ode, M. Ikeda, H. Murakami, and Y.H. Sohn

(Submitted September 28, 2008; in revised form January 9, 2009)

Ternary interdiffusion in $L1_2$-Ni$_3$Al with ternary alloying addition of Re was investigated at 1473 K using solid-to-solid diffusion couples. Interdiffusion flux of Ni, Al, and Re were directly calculated from experimental concentration profiles and integrated for the determination of average ternary interdiffusion coefficients. The magnitude of main interdiffusion coefficients $\tilde{\tilde{D}}_{NiNi}^{Al}$ and $\tilde{\tilde{D}}_{AlAl}^{Ni}$ was determined to be much larger than that of the main interdiffusion coefficient $\tilde{\tilde{D}}_{ReRe}^{Al(orNi)}$. A moderate tendency for Re to substitute for Al sites was reflected by its influence on interdiffusion of Al, quantified by large and positive $\tilde{\tilde{D}}_{AlRe}^{Ni}$ coefficients. Similar trends were observed from ternary interdiffusion coefficients determined by Boltzmann-Matano analysis. Profiles of concentrations and interdiffusion fluxes were also examined to estimate binary interdiffusion coefficients in Ni$_3$Al, and tracer diffusion coefficients of Re ($5.4\times10^{-16} \pm 2.3\times10^{-16}$ m^2/s) in Ni$_3$Al.

Keywords	high-temperature alloys, intermetallics, $L1_2$, Ni$_3$Al, Re, ternary interdiffusion

1. Introduction

Ni$_3$Al precipitation and the associated coherency through tetragonal distortion with the γ matrix is the key point behind the extensive use of Ni-base superalloys for high-temperature applications.[1] Multicomponent diffusion plays an important role in processing and degradation of these alloys that must possess exceptional high-temperature strength, microstructural stability, and oxidation resistance. Multicomponent diffusion mobility database[2] for γ phase, together with the alloying studies[3-10] to modify coherent precipitate (γ′) have yielded excellent design criteria to develop advanced superalloys. Recent development of refractory-based superalloys with $L1_2$ precipitates, and refractory-modified aluminide coatings[11-16] warrant a better understanding of interdiffusion in Ni$_3$Al with alloying additions.

The ordered crystal structure of Ni$_3$Al consists of face centers (α sites) occupied by Ni atoms and corners (β sites) of the unit cell occupied by Al atoms. Highly electronegative substitutional elements (e.g., Pt, Cu, and Co) occupy the α sites, whereas highly electropositive elements (e.g., Ti, Ta, and Nb) occupy the β sites in Ni$_3$Al.[1] The relative site preference for a ternary alloying element can be best illustrated from the direction of the solubility lobes for the γ′ phase on the ternary isotherm of Ni-Al-X (X = alloying addition) system at 1273 K as shown by Fig. 1.[17] Site preference of ternary alloying additions to Ni$_3$Al has attracted significant interest as this true solid solution accepts a considerable amount of third elements into solution.[18-22]

The alloying phenomenon ultimately plays an important role in enhancing the thermomechanical properties and high-temperature oxidation resistance of this intermetallic phase.[19-26] The substitutional ternary alloying additions to Ni$_3$Al was first classified by Guard and Westbrook[18] as Ni occupiers or Al occupiers or those with no preference. Several studies[27-29] have examined the change in site preference of alloying elements as a function of temperature and chemical composition of Ni$_3$Al.

The diffusion mechanism in ordered alloys is more complex than disordered solid solutions.[30] Diffusion can occur preferentially through α or β sites that Ni or Al atoms mainly occupy, respectively, and the diffusion coefficient largely depends on the alloy composition related to the degree of order.[31-33] While tracer diffusion studies in γ′ Ni$_3$Al are difficult since ^{26}Al is not readily available, self-diffusion of Ni and chemical/impurity diffusion in Ni$_3$Al binary and Ni$_3$Al-X ternary alloys (X = Ir, Ta, Pt, Nb, Mo, Cr, Fe, Ti) have been studied.[3-6] The temperature dependency of the diffusion for a ternary alloying addition is evident from Arrhenius rate law.[34-36] The β site occupiers have been observed to diffuse more slowly than the α-site occupiers.[30,37] In $L1_2$-ordered structure, each Ni atom is surrounded by 4 Al and 8 Ni atoms as nearest neighbors, where as an Al atom is surrounded by 12 Ni atoms as nearest neighbors. Consequently, the activation enthalpy of alloying elements can change because of the antisite-defect formation.[37]

To further understand the diffusion process in the $L1_2$ structure, to help improve the microstructural stability of Ni-base superalloys, and to help develop refractory-modified aluminide oxidation-resistant coatings, the authors examined the ternary diffusional interaction of Re additions

N. Garimella and **Y.H. Sohn**, Advanced Materials Processing and Analysis Center, Department of Mechanical, Materials and Aerospace Engineering, University of Central Florida, Orlando, FL, USA; **M. Ode** and **H. Murakami**, National Institute for Materials Science, Tsukuba, Japan; **M. Ikeda**, Kobe Steel, Co. Ltd., Kobe, Japan. Contact e-mail: ysohn@mail.ucf.edu.
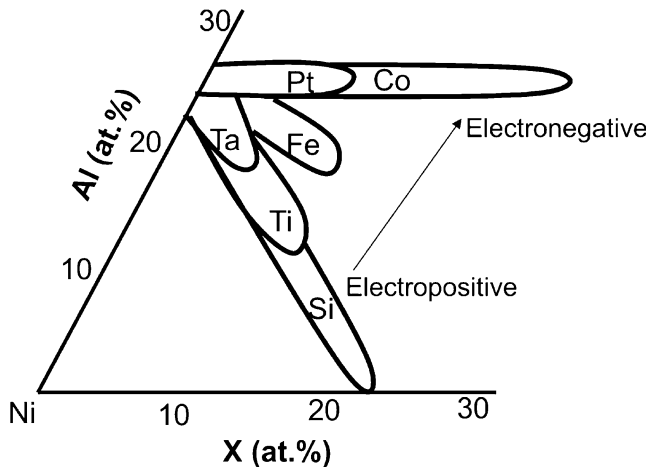
Fig. 1 Solubility ranges of selected ternary alloying additions in Ni$_3$Al at 1273 K[11]

to the $L1_2$ Ni$_3$Al phase. Solid-to-solid diffusion couples were assembled with various Ni$_3$Al-Re alloys and annealed at 1473 K for 5 h. Average ternary interdiffusion coefficients from an integration of interdiffusion fluxes and ternary interdiffusion coefficients via Boltzmann-Matano analysis were determined from concentration profiles obtained by electron probe microanalysis (EPMA). In addition, binary interdiffusion coefficients in Ni$_3$Al and tracer diffusion coefficients of Re in Ni$_3$Al were estimated.

2. Determination of Ternary Interdiffusion Coefficients

Based on Onsager's formalism[38,39] and Fick's law,[40] the interdiffusion flux $\tilde{J}_i$ of component i in a ternary system can be expressed in terms of two independent concentration gradients, $\partial C_j/\partial x$ by:

$$\tilde{J}_i = -\tilde{D}_{i1}^3 \frac{\partial C_1}{\partial x} - \tilde{D}_{i2}^3 \frac{\partial C_2}{\partial x} \quad (i = 1, 2) \qquad \text{(Eq 1)}$$

where $\tilde{D}_{ij}^3$ refers to the ternary interdiffusion coefficients. An experimental determination of the four concentration-dependent interdiffusion coefficients can be carried out by the use of Boltzmann-Matano analysis with two independent diffusion couples that develop a common composition in the diffusion zone where the interdiffusion coefficients can be evaluated.[41,42]

Instead, the interdiffusion flux at any section x can be calculated directly from the concentration profile from the relation[43,44]:

$$\tilde{J}_i = \frac{1}{2t} \int_{C_i^- \text{ or } C_i^+}^{C_i(x)} (x - x_o)dC_i \quad (i = 1, 2, \ldots, n) \qquad \text{(Eq 2)}$$

where t is the time, C_i^- and C_i^+ are the terminal concentrations, and x_o refers to the location of the Matano plane. Use of Eq 2 allows quantitative assessment of diffusional

behavior for any components including zero-flux-planes (ZFPs) and flux-reversals that can develop during multi-component interdiffusion.[43-46] In addition, the calculated interdiffusion fluxes can be related to interdiffusion parameters that can be employed to model and characterize concentration profiles.[47-50]

The interdiffusion flux $\tilde{J}_i$ determined from Eq 2 can be integrated over a selected region, x_1 to x_2, to yield an expression based on Eq 1[50]:

$$\int_{x_1}^{x_2} \tilde{J}_i dx = - \int_{C_1(x_1)}^{C_1(x_2)} \tilde{D}_{i1}^3 dC_1 - \int_{C_2(x_1)}^{C_2(x_2)} \tilde{D}_{i2}^3 dC_2 \quad (i = 1, 2)$$
$$= \bar{\bar{D}}_{i1}^3 [C_1(x_1) - C_1(x_2)]$$
$$+ \bar{\bar{D}}_{i2}^3 [C_2(x_1) - C_2(x_2)] \quad (i = 1, 2) \qquad \text{(Eq 3)}$$

where $\bar{\bar{D}}_{ij}^3$ corresponds to the *average* values of main and cross interdiffusion coefficients.

With $\bar{\bar{D}}_{ij}^3$ taken as constants, Eq 1 is re-written as:

$$\tilde{J}_i = -\bar{\bar{D}}_{i1}^3 \frac{\partial C_1}{\partial x} - \bar{\bar{D}}_{i2}^3 \frac{\partial C_2}{\partial x} \quad (i = 1, 2) \qquad \text{(Eq 4)}$$

If both sides of Eq 4 are multiplied by $(x - x_o)^m$ and integrated over the diffusion zone between x_1 and x_2, one obtains in general[50]:

$$\int_{x_1}^{x_2} \tilde{J}_i (x - x_o)^m dx = -\bar{\bar{D}}_{i1}^3 \int_{C_1(x_1)}^{C_1(x_2)} (x - x_o)^m dC_1$$
$$- \bar{\bar{D}}_{i2}^3 \int_{C_2(x_1)}^{C_2(x_2)} (x - x_o)^m dC_2 \quad (i = 1, 2)$$

$$\text{(Eq 5)}$$

If the exponent m is chosen to be zero, Eq 5 becomes identical to Eq 3. For $m = 1$, Eq 5 becomes[50]:

$$\int_{x_1}^{x_2} \tilde{J}_i (x - x_o)dx = -\bar{\bar{D}}_{i1}^3 \int_{C_1(x_1)}^{C_1(x_2)} (x - x_o)dC_1$$
$$- \bar{\bar{D}}_{i2}^3 \int_{C_2(x_1)}^{C_2(x_2)} (x - x_o)dC_2$$
$$= 2t \left\{ \bar{\bar{D}}_{i1}^3 [\tilde{J}_1(x_1) - \tilde{J}_1(x_2)] \right.$$
$$\left. + \bar{\bar{D}}_{i2}^3 [\tilde{J}_2(x_1) - \tilde{J}_2(x_2)] \right\} \quad (i = 1, 2)$$

$$\text{(Eq 6)}$$

Equations 3 and 6 provide four equations to solve for $\bar{\bar{D}}_{11}^3$, $\bar{\bar{D}}_{12}^3$, $\bar{\bar{D}}_{21}^3$, and $\bar{\bar{D}}_{22}^3$ and interdiffusion coefficients and can be easily set up from experimental concentrations and the corresponding interdiffusion fluxes. Thus, from the concentration profiles of a single diffusion couple, $\bar{\bar{D}}_{ij}^3$ $(i, j = 1, 2)$ coefficients, characteristic of the diffusion path, can be

determined over selected composition ranges in the diffusion zone.[50] This analysis method has been directly employed in various studies[51-59] to determine average ternary interdiffusion coefficients. In this paper, this analysis is applied to the experimental concentration profiles for two segments, one on either side of the Matano plane; the two chosen composition ranges are $(C_i^- - C_i^o)$ and $(C_i^o - C_i^+)$ where C_i^o refers to the concentration at the Matano plane. The average ternary interdiffusion coefficients, $\bar{\bar{D}}_{ij}^3$, determined on either side of the Matano plane, are employed to model experimental concentration profiles using error-function solution for infinite ternary system given by Fujita and Gosting.[60]

The uncertainty in the $\tilde{D}_{ij}^3$ values evaluated by the Boltzmann-Matano analysis arise mainly from the errors in the experimental determination of the concentration gradients of two of the components ($i = 1, 2$) at the common composition of a pair of couples with intersecting diffusion paths. These errors can be appreciable ($>100\%$), if the paths intersect at narrow angles and the concentration gradients of the components at the common compositions are comparable for the couple pair. On the other hand, the errors involved in the calculation of the integrals in Eq 3 and 6 of the present analysis are minimal and the errors in the determination of the $\bar{\bar{D}}_{ij}^3$ values reported in this paper are estimated for $\bar{\bar{D}}_{ij}^3$ to be less than 20% based on assumed uncertainties in concentrations of 3 at.%.[50]

3. Experimental Details

Ni-Al and Ni-Al-Re alloys were prepared by the vacuum arc melting of 99.97 wt.% Ni, 99.9 wt.% Al, and 99.2 wt.% Re, according to the compositions presented in Table 1. The alloys were cast into a semicylindrical mold with the diameter of 8 mm. The alloy rods were homogenized at 1473 K for 137 h in the vacuum furnace that was evacuated

Table 1 Nominal composition of alloys employed for diffusion couple studies

Alloy identification	Composition, at.%			Composition, wt.%		
	Ni	Al	Re	Ni	Al	Re
Ni-24.5Al	75.5	24.5	0.0	58.6	41.4	0.0
Ni-25Al	75.0	25.0	0.0	57.9	42.1	0.0
Ni-26Al	74.0	26.0	0.0	56.7	43.3	0.0
Ni-23.5Al-0.5Re	76.0	23.5	0.5	59.7	40.2	0.1
Ni-23.5Al-0.7Re	75.8	23.5	0.7	59.6	40.2	0.2

Table 2 Diffusion couples assembled and analyzed after an anneal at 1473 K for 5 h

Ni-24.5Al vs. Ni-23.5Al-0.5Re
Ni-24.5Al vs. Ni-23.5Al-0.7Re
Ni-25Al vs. Ni-23.5Al-0.5Re
Ni-26Al vs. Ni-23.5Al-0.7Re

to a pressure lower than 10^{-2} Pa. A thorough metallographic characterization with x-ray diffusion was carried out to confirm that all alloys reported in Table 1 were free of any second phase. The homogenized alloys were then sectioned into disks with an approximate height of 1.5 mm.
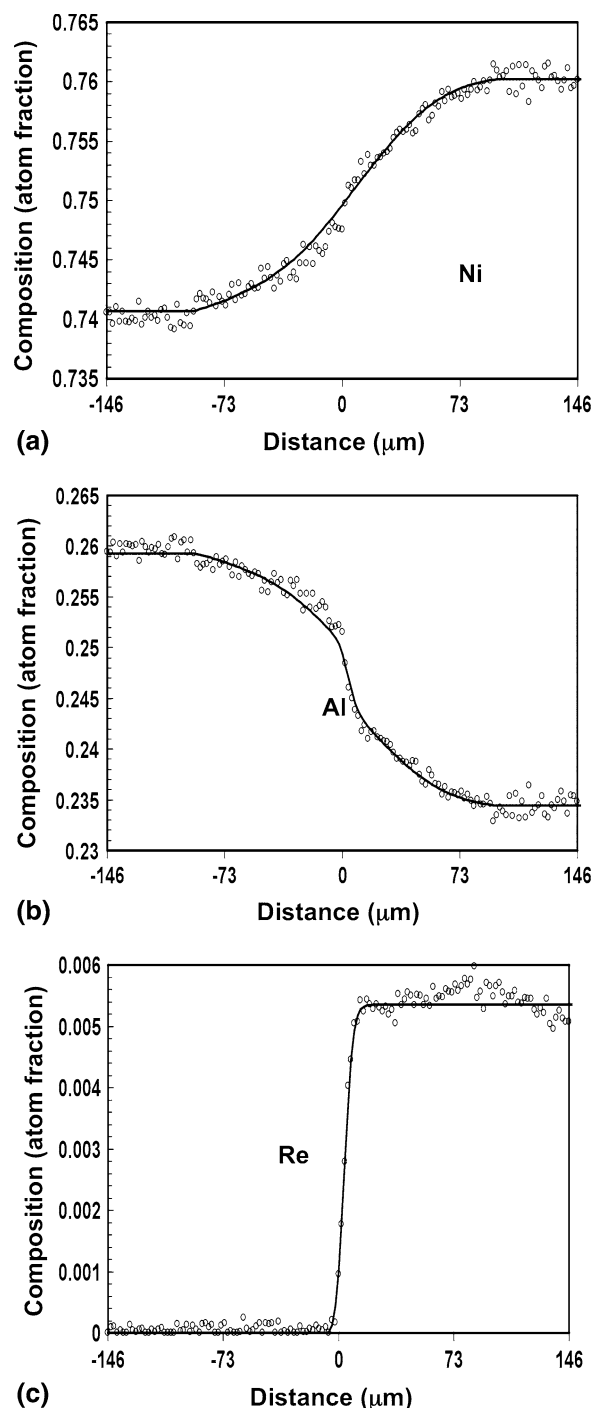

Fig. 2 Concentration profiles of (a) Ni, (b) Al, and (c) Re obtained from diffusion couple Ni-25Al vs. Ni-23.5Al-0.5Re annealed at 1473 K for 5 h. Open circles and solid lines represent EPMA measurement and calculated concentration profiles, respectively

The surfaces of alloy disks were ground metallographically down to 1200 grit and cleaned thoroughly prior to diffusion couple assembly.

Table 2 presents diffusion couples that were assembled and analyzed in this study. To promote initial bonding, coupled alloys were placed in a Si_3N_4 jig and annealed at 1473 K for 0.5 h in a vacuum furnace. The metal disks have larger thermal expansion coefficients than the Si_3N_4 jig, and the discs can adhere to each other because of the compression during the annealing treatment. Each diffusion couple fabricated in this manner was then sealed in an evacuated transparent quartz capsule and annealed at 1473 K for 4.5 h in an atmosphere furnace. All diffusion couples were water quenched after the high-temperature anneal to preserve high-temperature microstructure and concentrations. In this study, the time required for the diffusion bonding treatment (0.5 h) was added to the total annealing time. Thus, concentration profiles from all diffusion couples were analyzed with diffusion anneal time of 5 h.

Microstructural analysis by optical microscopy confirmed excellent bonding in all diffusion couples without any precipitation of other phases. Concentration profiles of the annealed diffusion couples were analyzed by JEOL-JXA-8900 EPMA. An accelerating voltage of 20 keV, a beam current of 50 nA, and a probe diameter of 1 μm were used for data acquisition of Ni Kα x-radiation peak using lithium fluoride (LiF) crystal, Al Kα x-radiation peak using thallium acid phthalate (TAP) crystal, and Re Lα x-radiation using LiFH crystal. Elemental standards of Ni, Al, and Re along with ZAF[61] correction were used for quantification of concentrations via point-to-point count technique. JEOL-JXA-8900 EPMA has a secondary electron resolution of 3 nm, and its uncertainty in concentration measurement is within ±0.1 at.%.

4. Results and Analysis

4.1 Profiles of Concentrations and Interdiffusion Fluxes

Figure 2 presents typical concentration profiles obtained by EPMA from the diffusion couple, Ni-25Al versus Ni-23.5Al-0.5Re annealed at 1473 K for 5 h. The x-axis is the distance from the Matano plane, and the open circles represent EPMA measurement. Scatter in the concentration profiles for all diffusion couples were minimum and within the experimental uncertainty associated with EPMA. The interdiffusion fluxes of individual components were then determined using Eq 2 from experimental concentration profiles that were smoothened with a series of weighted splines. Although no zero-flux plane was observed, a significant diffusional interaction between Al and Re was observed when Ni_3Al was diffusion annealed against Ni_3Al alloyed with Re. As shown in Fig. 2, interdiffusion of Al was reduced by the interdiffusion of Re against the gradient of Al. However, the diffusional influence of Re on Ni is difficult to ascertain from the profiles presented in Fig. 2. Determination of ternary interdiffusion coefficients can quantify the extent of these diffusional interactions and provide competent approaches to compositional design and modification of alloys and protective coatings.

4.2 Average Ternary Interdiffusion Coefficients

From profiles of concentration and interdiffusion fluxes in Ni-Al versus Ni-Al-Re diffusion couples, average ternary interdiffusion coefficients, $\bar{\bar{D}}_{ij}^{Ni}$ $(i,j = Al, Re)$ and $\bar{\bar{D}}_{ij}^{Al}$ $(i,j = Ni, Re)$ were determined on either side of the Matano plane using Eq 3 and 6. They are reported in Table 3. The magnitudes of main diffusion coefficients, $\bar{\bar{D}}_{AlAl}^{Ni}$ and $\bar{\bar{D}}_{NiNi}^{Al}$ are similar to the interdiffusion coefficients of Al and Ni reported in literature for binary Ni_3Al at 1473 K.[3-10] Estimation of binary interdiffusion coefficients from the ternary diffusion couples and the comparison to the interdiffusion coefficients of Al and Ni reported in literature for binary Ni_3Al are presented in detail in section 4.4. The main interdiffusion coefficient, $\bar{\bar{D}}_{ReRe}$ is approximately 100 times smaller in magnitude than $\bar{\bar{D}}_{AlAl}^{Ni}$ and $\bar{\bar{D}}_{NiNi}^{Al}$. Table 3 reports that $\bar{\bar{D}}_{AlRe}^{Ni}$ coefficients are positive and comparable to the magnitude of $\bar{\bar{D}}_{AlAl}^{Ni}$, while $\bar{\bar{D}}_{ReAl}^{Ni}$ coefficients are negligibly small $(<0.1 \times 10^{-16} \ m^2/s)$. Thus, the interdiffusion of Al can be strongly influenced by the

Table 3 Average ternary interdiffusion coefficients determined from Ni-Al vs. Ni-Al-Re diffusion couples annealed at 1473 K for 5 h

Diffusion couple	Composition range	Composition at x_o, at.%	Average ternary interdiffusion coefficients, $10^{-16} \ m^2/s$							
			$\bar{\bar{D}}_{AlAl}^{Ni}$	$\bar{\bar{D}}_{AlRe}^{Ni}$	$\bar{\bar{D}}_{ReAl}^{Ni}$	$\bar{\bar{D}}_{ReRe}^{Ni}$	$\bar{\bar{D}}_{NiNi}^{Al}$	$\bar{\bar{D}}_{NiRe}^{Al}$	$\bar{\bar{D}}_{ReNi}^{Al}$	$\bar{\bar{D}}_{ReRe}^{Al}$
Ni-24.5Al vs. Ni-23.5Al-0.5Re	$(C_i^{-\infty}$ to $C_i^o)$	75.5Ni-24.3Al-0.3Re	417.7	380.2	Ngl	3.8	417.7	33.7	Ngl	3.8
	$(C_i^o$ to $C_i^{+\infty})$		265.1	191.0	Ngl	4.0	265.1	70.1	Ngl	4.0
Ni-24.5Al vs. Ni-23.5Al-0.7Re	$(C_i^{-\infty}$ to $C_i^o)$	75.6Ni-24.1Al-0.3Re	509.9	463.4	Ngl	4.5	509.9	42.0	Ngl	4.5
	$(C_i^o$ to $C_i^{+\infty})$		362.8	304.1	Ngl	3.4	362.8	55.3	Ngl	3.4
Ni-25Al vs. Ni-23.5Al-0.5Re	$(C_i^{-\infty}$ to $C_i^o)$	75.3Ni-24.4Al-0.3Re	463.2	294.6	Ngl	3.8	463.2	164.8	Ngl	3.8
	$(C_i^o$ to $C_i^{+\infty})$		668.3	477.4	Ngl	2.4	668.3	188.5	Ngl	2.4
Ni-26Al vs. Ni-23.5Al-0.7Re	$(C_i^{-\infty}$ to $C_i^o)$	74.9Ni-24.8Al-0.3Re	449.9	336.6	Ngl	5.8	449.9	107.5	Ngl	5.8
	$(C_i^o$ to $C_i^{+\infty})$		298.9	123	Ngl	4.7	298.9	171.2	Ngl	4.7

Note: Ngl refers to magnitude less than $0.1 \times 10^{-16} \ m^2/s$

interdiffusion of Re. The $\bar{\bar{D}}_{\text{NiRe}}^{\text{Al}}$ coefficients are also positive, but 2 to 13 times smaller in magnitude than the $\bar{\bar{D}}_{\text{NiNi}}^{\text{Al}}$.

The average ternary interdiffusion coefficients reported in Table 3 were used to generate concentration profiles using the error-function solution provided by Fujita and Gosting.[60] Excellent agreement between EPMA measurement and calculated concentration profiles were found for all couples. Typical examples are presented in Fig. 2 where open circles are the EPMA data, and solid lines are the calculated concentration profiles.

4.3 Ternary Interdiffusion Coefficients Determined by Boltzmann-Matano Analysis

From the diffusion couples Ni-Al versus Ni-Al-Re listed in Table 2, several intersecting compositions were found within the diffusion paths. Intersecting diffusion paths in Fig. 3 represent typical diffusion paths with one of the paths intersecting with its terminal end. In other words, Re concentration of that end remained constant with no concentration gradient. These intersection composition points may be used for the determination of interdiffusion coefficients using Boltzmann-Matano analysis. Uncertainty in ternary interdiffusion coefficients determined by Boltzmann-Matano analysis is higher than aforementioned in section 2 because of the low angle of intersecting paths combined with uncertainty in the measurement of concentration gradients. Nevertheless, the values of ternary interdiffusion coefficients determined in this study are reported in Table 4 and have the same order of magnitude when compared to average ternary interdiffusion coefficients presented in Table 3. The slight deviation in values and change in signs of the $\bar{\bar{D}}_{\text{NiRe}}^{\text{Al}}$ coefficients are attributed to the uncertainty in concentration gradient of Re.

4.4 Estimation of Binary Interdiffusion Coefficients in Ni₃Al

The ternary interdiffusion coefficients $\tilde{D}_{\text{AlAl}}^{\text{Ni}}$ and $\tilde{D}_{\text{NiNi}}^{\text{Al}}$ approach the binary $\tilde{D}_i$ for Ni₃Al as the concentration of Re decreases to zero. Hence, values of $\tilde{D}_i$ ($i = $ Ni or Al) were estimated from ternary diffusion couples where Re concentration was negligibly small in segments of the diffusion zone (e.g., Fick's law for substitutional binary alloys). Such regions were found in all couples since $\bar{\bar{D}}_{\text{ReRe}}$ coefficients are much smaller than $\bar{\bar{D}}_{\text{AlAl}}^{\text{Ni}}$ and $\bar{\bar{D}}_{\text{NiNi}}^{\text{Al}}$. The $\tilde{D}_i$ coefficients extrapolated from the ternary couples with large enough concentration difference (e.g., ΔC_{Al} or $\Delta C_{\text{Ni}} > 2$ at.%) in terminal alloys is presented in Fig. 4. These values appear consistent with the available binary interdiffusion data[3-10] for Ni₃Al.

4.5 Estimation of Tracer Diffusion Coefficient of Re in Ni₃Al

For a ternary component i diffusing into a binary alloy j-k, the cross interdiffusion coefficient $\tilde{D}_{ij}^k$ ($i \neq j$) becomes negligible at infinite dilution of component i in a j-k alloy.[62] Then the value of the main coefficient $\tilde{D}_{ii}$
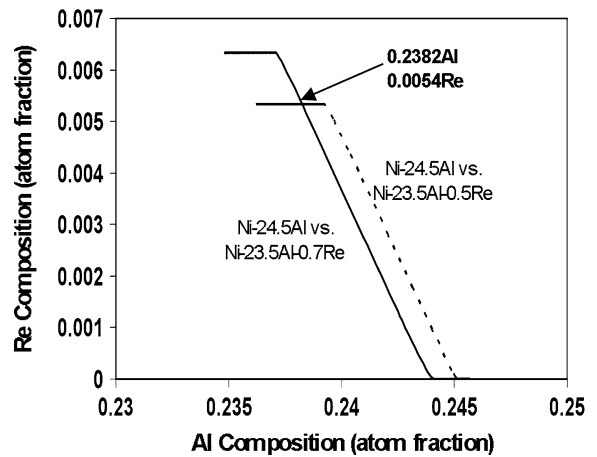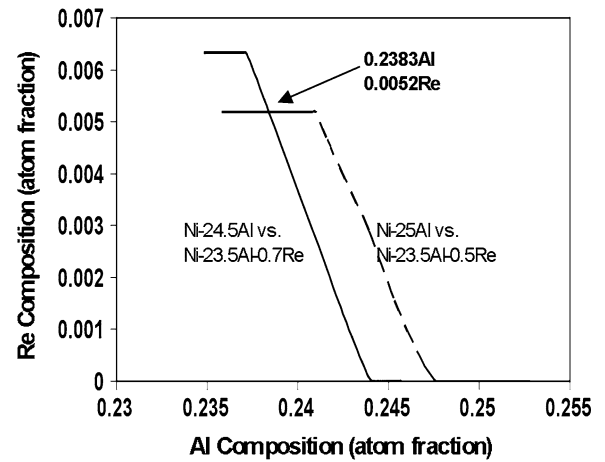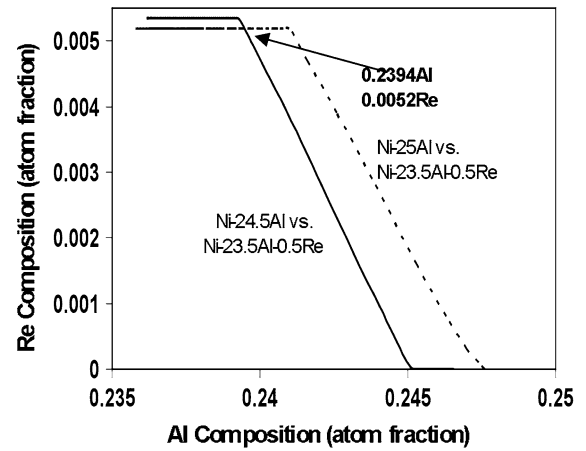

Fig. 3 Typical intersecting diffusion paths of Ni-Al vs. Ni-Al-Re diffusion couples annealed at 1473 K for 5 h. Compositions at these intersections were used for the determination of ternary interdiffusion coefficients based on Boltzmann-Matano analysis

approaches that of the tracer diffusion coefficient D_i^* for component i:

$$C_i \to 0 \quad \tilde{J}_i = -\tilde{D}_{ii}^k \frac{\partial C_i}{\partial x} \cong -D_{i(jk)}^* \frac{\partial C_i}{\partial x} \qquad \text{(Eq 7)}$$

Table 4 Ternary interdiffusion coefficients determined by Boltzmann-Matano analysis from Ni-Al vs. Ni-Al-Re diffusion couples annealed at 1473 K for 5 h

Diffusion couples with intersecting diffusion paths	Intersecting composition, at.%	Ternary interdiffusion coefficients, 10^{-16} m^2/s							
		$\tilde{D}_{AlAl}^{Ni}$	$\tilde{D}_{AlRe}^{Ni}$	$\tilde{D}_{ReAl}^{Ni}$	$\tilde{D}_{ReRe}^{Ni}$	$\tilde{D}_{NiNi}^{Al}$	$\tilde{D}_{NiRe}^{Al}$	$\tilde{D}_{ReNi}^{Al}$	$\tilde{D}_{ReRe}^{Al}$
Ni-24.5Al vs. Ni-23.5Al-0.5Re, Ni-25Al vs. Ni-23.5Al-0.5Re	Al: 0.239, Re: 0.005	832.5	926.5	Ngl	2.8	832.5	−96.8	Ngl	2.8
Ni-24.5Al vs. Ni-23.5Al-0.5Re, Ni-24.5Al vs. Ni-23.5Al-0.7Re	Al: 0.2382, Re: 0.005	244.2	216.0	Ngl	3.1	244.2	25.0	Ngl	3.1
Ni-25Al vs. Ni-23.5Al-0.5Re, Ni-24.5Al vs. Ni-23.5Al-0.7Re	Al: 0.2393, Re: 0.005	726.1	734.9	Ngl	3.1	726.1	−11.9	Ngl	3.1

Note: Ngl refers to magnitude less than 0.1×10^{-16} m^2/s. Values reported contain high uncertainty due to low angle of intersecting paths combined with uncertainty in the measurement of concentration gradients
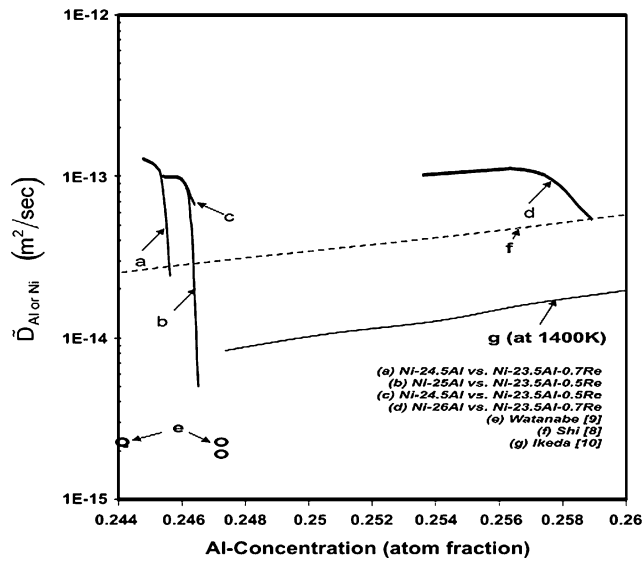

Fig. 4 Interdiffusion coefficients in Ni$_3$Al at 1473 K compiled from this investigation and literature review

Fig. 5 Extrapolation of $\tilde{D}_{ReRe}$ coefficient for the estimation of tracer diffusion coefficient of Re in Ni$_3$Al at 1473 K

Thus, the tracer diffusion coefficients of Re in Ni$_3$Al alloy can be estimated from the main interdiffusion coefficient of Re, $\tilde{D}_{ReRe}^{Ni(or)Al}$, using Eq 7, provided the concentration of Re approaches zero within the diffusion zone so that the cross-interdiffusion coefficients, $\tilde{D}_{ReAl}^{Ni}$ or $\tilde{D}_{ReNi}^{Al}$, become negligible. Such regions were found in all couples since $\tilde{D}_{ReRe}$ coefficients are much smaller than $\tilde{D}_{AlAl}^{Ni}$ and $\tilde{D}_{NiNi}^{Al}$. Values of tracer diffusion coefficients of Re, D_{Re}^{*} were extrapolated from the main interdiffusion coefficients, $\tilde{D}_{ReRe}^{Ni}$ or $\tilde{D}_{ReRe}^{Al}$ as the concentration of Re, becomes zero. The extrapolations for D_{Re}^{*} from the ternary interdiffusion coefficients on the basis of Eq 7 are presented in Fig. 5 for Ni-24.4Al to Ni-24.8Al (at.%). The estimated values of D_{Re}^{*} are reported in Table 5.

5. Concluding Remarks

Ternary interdiffusion interactions of Re addition on the $L1_2$ Ni$_3$Al phase were examined using solid-to-solid
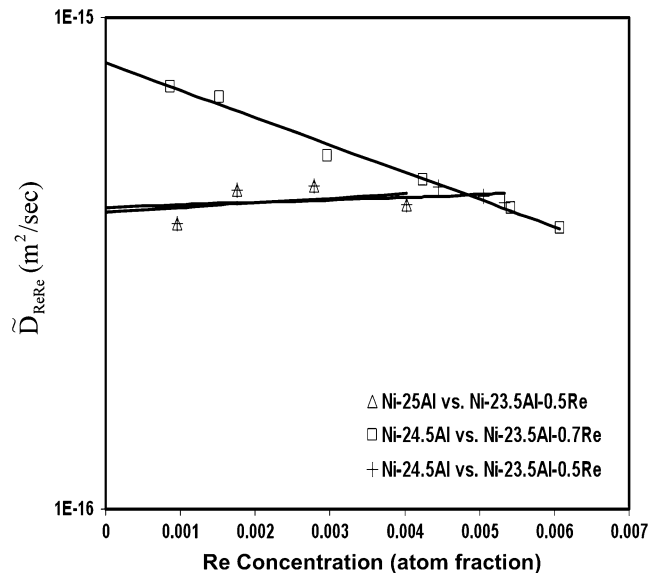
Table 5 Tracer diffusion coefficients of Re in Ni$_3$Al extrapolated from ternary interdiffusion coefficients of diffusion couples annealed at 1473 K

Composition	Tracer component	D_i^{*}, 10^{-16} m^2/s
75.2Ni-24.8Al	Re	4.0
75.6Ni-24.4Al	Re	8.1
75.5Ni-24.5Al	Re	4.1
Average values		5.4 ± 2.3

diffusion couples annealed at 1473 K for 5 h. Average ternary interdiffusion coefficients were determined from an integration of interdiffusion fluxes for individual components. The magnitude of $\tilde{D}_{NiNi}^{Al}$ and $\tilde{D}_{AlAl}^{Ni}$ coefficients was determined to be much larger than that of $\tilde{D}_{ReRe}$ coefficients. The $\tilde{D}_{AlRe}^{Ni}$ coefficient was determined to be positive and large in magnitude; Re substitutes in Al site and influences

the interdiffusion of Al significantly. The $\bar{\bar{D}}_{\mathrm{NiRe}}^{\mathrm{Al}}$ coefficient was also positive but relatively low in magnitude; Re shows a lower tendency to occupy Ni sites. Consistency among ternary interdiffusion coefficients was observed from ternary interdiffusion coefficients determined by Boltzmann-Matano analysis. Profiles of concentrations were also examined to estimate binary interdiffusion coefficients in Ni$_3$Al. Tracer diffusion coefficient of Re at 1473 K was also estimated as $D_{\mathrm{Re}}^{*} = 5.4 \times 10^{-16} \pm 2.3 \times 10^{-16}\,\mathrm{m^2/s}$ for Ni$_3$Al phase with Al concentration range of 24.4 to 24.8 at.%.

Acknowledgments

Open Access

References

1. C.T. Sims, N.S. Stoloff, and W.C. Hagel, *Superalloys II*, John Wiley & Sons, New York, 1987
2. C.E. Campbell, W.J. Boettinger, and U.R. Kattner, Development of a Diffusion Mobility Database for Ni-Base Superalloys, *Acta Mater.*, 2002, **50**(4), p 775-792
3. N. Garimella, M. Ode, M. Ikeda, H. Murakami, and Y.H. Sohn, Effects of Ir and Ta Alloying Addition on Interdiffusion of *L*1$_2$-Ni$_3$Al, *Intermetallics*, 2008, **16**(9), p 1095-1103
4. J. Cermak and V. Rothova, Concentration Dependence of Ternary Interdiffusion Coefficients in Ni$_3$Al/Ni$_3$Al-X Couples with X = Cr, Fe, Nb and Ti, *Acta Mater.*, 2003, **51**(15), p 4411-4421
5. V. Rothova and J. Cermak, Bulk and Grain Boundary Diffusion of ^{67}Ga in Ni$_3$Al Influence of Composition, *Intermetallics*, 2005, **13**(1), p 113-120
6. Y. Minamino, H. Yoshida, S.B. Jung, K. Hirao, and T. Yamane, Diffusion of Platinum and Molybdenum in Ni and Ni$_3$Al, *Defect Diff. Forum*, 1997, **143-147**, p 257-262
7. M.M.P. Janssen, Diffusion in the Nickel-Rich Part of the Ni-Al System at 1000° to 1300°C, Ni3Al Layer Growth, Diffusion Coefficients and Interface Concentrations, *Metall. Trans.*, 1973, **4**(6), p 1623-1633
8. Y. Shi, G. Frohberg, and H. Wever, Diffusion of Ni and In in the γ′-phase Ni$_3$Al, *Phys. Status Solidi A*, 1995, **152**(2), p 361-375
9. M. Watanabe, Z. Horita, D.J. Smith, M.R. McCartney, T. Sano, and M. Nemoto, Electron Microscopy Study of Ni/Ni[3]Al Diffusion-Couple Interface. II: Diffusivity Measurement, *Acta Metall. Mater.*, 1994, **42**(10), p 3389-3396
10. T. Ikeda, A. Almazouzi, H. Numakura, M. Koiwa, W. Sprengel, and H. Nakajima, Single-Phase Interdiffusion in Ni$_3$Al, *Acta Mater.*, 1998, **46**(15), p 5369-5376
11. Y.N.A. Wu, J. Tsukuba, A. Yamaguchi, J. Tsukuba, and S. Kuroda, Role of Iridium in Hot Corrosion Resistance of Pt-Ir Modified Aluminide Coatings with Na$_2$SO$_4$-NaCl Salt at 1173 K, *Mater. Trans.*, 2006, **47**(8), p 1918-1921
12. T. Abe, M. Ode, H. Murakami, C.S. Oh, C. Kocer, Y. Yamabe-Mitarai, and H. Onodera, A Thermodynamic Description of the Al-Ir System, *Mater. Sci. Forum*, 2007, **539-543**(3), p 2389-2394
13. H. Murakami, A. Yamaguchi, Y.N. Wu, and S. Kuroda, Effect of Hf Addition on High Temperature Properties of Ir-Containing Alloy Coatings, *Mater. Sci. Forum*, 2007, **546-549**(3), p 1689-1694
14. Y.N. Wu, A. Yamaguchi, H. Murakami, and S. Kuroda, Hot Corrosion Behavior of Pt-Ir Modified Aluminide Coatings on the Nickel-Base Single Crystal Superalloy TMS-82+, *J. Mater. Res.*, 2007, **22**(1), p 206-216
15. Y. Yamabe-Mitarai, T. Aoyagi, K. Nishida, H. Aoki, T. Abe, and H. Murakami, Phase Equilibria between the B2, L1$_2$, and fcc Phases in the Ir-Ni-Al System, *Intermetallics*, 2007, **15**(4), p 479-488
16. A. Suzuki, Y.N. Wu, A. Yamaguchi, H. Murakami, and C.M.F. Rae, Oxidation Behavior of Pt-Ir Modified Aluminized Coatings on Ni-base Single Crystal Superalloy TMS-82+, *Oxid. Met.*, 2007, **68**(1-2), p 53-64
17. S. Ochiai, Y. Oya, and T. Suzuki, Alloying Behaviour of Ni$_3$Al, Ni$_3$Ga, Ni$_3$Si and Ni$_3$Ge, *Acta Metall.*, 1984, **32**, p 289-298
18. R.W. Guard and J.H. Westbrook, Alloying Behaviour of Ni$_3$Al (γ′ Phase), *Trans. TMS-AIME*, 1959, **215**, p 807-814
19. R.F. Decker and J.R. Mihalisin, Coherency Strains in γ Hardened Nickel Alloys, *Trans. ASM*, 1969, **62**, p 481-489
20. R.D. Rawlings and A.E. Staton-Bevan, The Alloying Behaviour and Mechanical Properties of Polycrystalline Ni$_3$Al (γ′ Phase) with Ternary Additions, *J. Mater. Sci.*, 1975, **10**(3), p 505-514
21. A. Chiba, D. Shindo, and S. Watanabe, Site Occupation Determination of Pd in Ni$_3$Al, *Acta. Metall. Mater.*, 1991, **39**(1), p 13-18
22. A. Chiba, S. Hanada, and S. Watanabe, Effect of γ and γ′ Former Doping on Ductility of Ni$_3$Al, *Scr. Metall.*, 1991, **25**(2), p 303-307
23. A. Chiba, S. Hanada, and S. Watanabe, Correlation between Ductility and Ordering Energy of Ni$_3$Al, *Mater. Trans., JIM*, 1990, **31**(9), p 824-827
24. A. Chiba, S. Hanada, and S. Watanabe, Ductilization of Ni$_3$Al by Microalloying with Ag, *Scr. Mater.*, 1992, **26**(7), p 1031-1036
25. A. Chiba, S. Hanada, and S. Watanabe, Improvement in Ductility of Ni$_3$Al by γ Former Doping, *Mater. Sci. Eng. A*, 1992, **152**(1-2), p 108-113
26. B. Gleeson, W. Wang, S. Hayashi, and D. Sordelet, Effects of Platinum on the Interdiffusion and Oxidation Behavior of Ni-Al-Based Alloys, *Mater. Sci. Forum*, 2004, **461-464**, p 213-222
27. M.H.F. Sluiter and Y. Kawazoe, Site Preference of Ternary Additions in Ni$_3$Al, *Phys. Rev. B*, 1995, **51**(7), p 4062-4073
28. A.V. Ruban and H.L. Skriver, Calculated Site Substitution in Ternary γ′-Ni$_3$Al: Temperature and Composition Effects, *Phys. Rev. B*, 1997, **55**(14), p 8801-8807
29. M. Enomoto and H. Harada, Analysis of γ′/γ Equilibrium in Ni-Al-X Alloys by the Cluster Variation Method with the

Lennard-Jones Potential, *Metall. Mater. Trans. A*, 1989, **20**(4), p 649-664

30. H. Mehrer, Diffusion in Intermetallics, *Mater. Trans. JIM*, 1996, **37**(6), p 1259-1280

31. H. Numakura, T. Ikeda, M. Koiwa, and A. Almazouzi, Physics of Condensed Matter, Structure, Defects and Mechanical Properties, *Philos. Mag. A*, 1998, **77**(4), p 887-909

32. S.V. Divinski, S. Frank, U. Sodervall, and C. Herzig, Solute Diffusion of Al-Substituting Elements in Ni_3Al and the Diffusion Mechanism of the Minority Component, *Acta Mater.*, 1998, **46**(12), p 4369-4380

33. H. Numakura, T. Ikeda, H. Nakajima, and M. Koiwa, Diffusion in Ni_3Al, Ni_3Ga and Ni_3Ge, *Mater. Sci. Eng. A*, 2001, **312**(1-2), p 109-117

34. Y. Minamino, S.B. Jung, T. Yamane, and K. Hirao, Diffusion of Cobalt, Chromium, and Titanium in Ni_3Al, *Metall. Mater. Trans. A*, 1992, **23**(10), p 2783-2790

35. Y. Minamino, T. Yamane, S. Saji, K. Hirao, S.B. Jung, and T. Kohira, Diffusion of Copper, Iron and Silicon in $L1_2$-Type Intermetallic Compound Ni_3Al, *J. Jpn. Inst. Met.*, 1994, **58**(4), p 397-403

36. S.B. Jung, Y. Minamino, and T. Yamane, Diffusion of Mn in Ni and Ni_3Al, *J. Mater. Sci. Lett.*, 1999, **18**(13), p 1063-1066

37. J. Cermak, A. Gazda, and V. Rothova, Interdiffusion in Ternary Ni_3Al/Ni_3Al-X Diffusion Couples with X = Cr, Fe, Nb and Ti, *Intermetallics*, 2003, **11**(9), p 939-946

38. L. Onsager, Reciprocal Relations in Irreversible Processes, *Phys. Rev.*, 1931, **37**, p 405-426 and 1932, **38**, p 2265-2279

39. L. Onsager, The Diffusion of Electrolytes and Macromolecules in Solution, *Ann. NY Acad. Sci.*, 1965, **46**, p 241-265

40. A. Fick, Uber Diffusion, *Ann. Phys.*, 1855, **170**(1), p 59-86

41. J.S. Kirkaldy, Diffusion in Multicomponent Metallic Systems. I. Phenomenological Theory for Substitutional Solid-Solution Alloys, *Can. J. Phys.*, 1958, **36**, p 899-906

42. J.S. Kirkaldy and D.J. Young, *Diffusion in the Condensed State*, The Institute of Metals, London, 1987, p 226-272

43. M.A. Dayananda and C.W. Kim, Zero-Flux Planes and Flux Reversals in Copper-Nickel-Zinc Diffusion Couples, *Metall. Mater. Trans. A*, 1979, **10**(9), p 1333-1339

44. M.A. Dayananda, An Analysis of Concentration Profiles for Fluxes. Diffusion Depths, and Zero-Flux Planes in Multicomponent Diffusion, *Metall. Mater. Trans. A*, 1983, **14**(9), p 1851-1858

45. C.W. Kim and M.A. Dayananda, Identification of Zero-Flux Planes and Flux Reversals in Several Studies of Ternary Diffusion, *Metall. Mater. Trans. A*, 1983, **14**(5), p 857-864

46. C.W. Kim and M.A. Dayananda, Zero-Flux Planes and Flux Reversals in the Copper-Nickel-Zinc System at 775°, *Metall. Mater. Trans. A*, 1984, **15**(4), p 649-659

47. M.A. Dayananda and D.A. Behnke, Effective Interdiffusion Coefficients and Penetration Depths, *Scr. Metall.*, 1991, **25**(9), p 2187-2191

48. M.A. Dayananda, Average Effective Interdiffusion Coefficients and the Matano Plane Composition, *Metall. Mater. Trans. A*, 1996, **27**(9), p 2504-2509

49. M.A. Dayananda and Y.H. Sohn, Average Effective Interdiffusion Coefficients and Their Applications for Isothermal Multicomponent Diffusion Couples, *Scr. Mater.*, 1996, **35**(6), p 683-688

50. M.A. Dayananda and Y.H. Sohn, A New Analysis for the Determination of Ternary Interdiffusion Coefficients from a Single Diffusion Couple, *Metall. Mater. Trans. A*, 1999, **30**(3), p 535-543

51. M.S.A. Karunaratne, P. Carter, and R.C. Reed, On the Diffusion of Aluminum and Titanium in the Ni-rich Ni-Al-Ti System between 900 and 1200°C, *Acta Mater.*, 2001, **49**(5), p 861-875

52. R. Bouchet, R. Mevrel, and A. Numerical, Inverse Method for Calculating the Interdiffusion Coefficients Along a Diffusion Path in Ternary Systems, *Acta Mater.*, 2002, **50**(19), p 4887-4900

53. T. Morimura, M. Hasaka, and A. Nagata, Ordered Phase Formation and Diffusion Composition Path in Cu_3Au/Pd Couple, *J. Alloys Compd.*, 2002, **347**(1-2), p 141-148

54. R. Bachorczyk, M. Danielewski, and R. Filipek, Interdiffusion under the Chemical Potential Gradient; Comparison of Onsager and Darken Models, *Defect Diff. Forum*, 2003, **216-217**, p 141-147

55. J. Moon, P. Wynblatt, S. Garoff, and R. Suter, Pseudopartial Wetting and Precursor Film Growth in Immiscible Metal Systems, *Surf. Sci.*, 2004, **559**(2-3), p 149-157

56. P. Dawah-Tankeu, L. Dorer, G. Borchardt, K. Gomann, W.M. Pragnell, H.E. Evans, and J.L. Coze, Concentration Dependence of the Ternary Interdiffusivities in the FeCrAl System at 1100 °C, *Mater. High Temp.*, 2005, **22**(3-4), p 375-384

57. N. Garimella, M.P. Brady, and Y.H. Sohn, Interdiffusion in γ (Face-Centered Cubic) Ni-Cr-X (X = Al, Si, Ge, or Pd) Alloys at 900°C, *J. Phase. Equilib. Diffus.*, 2006, **27**(6), p 665-670

58. S. Kim and J.H. Perepezko, Interdiffusion Kinetics in the Mo_5SiB_2 (T_2) Phase, *J. Phase Equilib. Diffus.*, 2006, **27**(6), p 605-613

59. L.R. Ram-Mohan and M.A. Dayananda, A Transfer Matrix Method for the Calculation of Concentrations and Fluxes in Multicomponent Diffusion Couples, *Acta Mater.*, 2006, **54**(9), p 2325-2334

60. H. Fujita and L.J. Gosting, An Exact Solution of the Equations for Free Diffusion in Three-Component Systems with Interacting Flows, and its Use in Evaluation of the Diffusion Coefficients, *J. Am. Chem. Soc.*, 1956, **78**(6), p 1099-1106

61. J.L. Pouchou and F. Pchoir, A New Model for Quantitative X-ray Microanalysis. I. Application to the Analysis of Homogeneous Samples, *Recherche Aerosp.*, 1984, **3**, p 13-38

62. T.O. Ziebold and R.E. Ogilvie, Ternary Diffusion in Copper-Silver-Gold Alloys, *Trans. TMS-AIME*, 1967, **239**(7), p 942-953